

Processing Conditions and Aging Effect on the Morphology of PZT Electrospun Nanofibers, and Dielectric Properties of the Resulting 3–3 PZT/Polymer Composite

Ebru Mensur Alkoy,[†] Canan Dagdeviren, and Melih Papila

Faculty of Engineering and Natural Sciences, Sabanci University, Tuzla, Istanbul 34956, Turkey

Lead zirconate titanate (PZT) nanofibers are obtained by electrospinning a sol–gel based solution and polyvinyl pyrrolidone (PVP) polymer, and by subsequent sintering of the electrospun precursor fibers. The average diameter of the precursor PZT/PVP green fibers has increased with the aging of the precursor solution along with an increase in the viscosity. Bead-free uniform green PZT/PVP fibers were collected at about an ~ 230 nm average fiber diameter using a 28 wt% PVP ratio solution with a viscosity of 290 mPa. Shrinkage of 40% was recorded on the fiber diameter after sintering. The X-ray diffraction pattern of the annealed PZT fibers exhibits no preferred orientation and a perovskite phase. Preparation of 3–3 nanocomposites by the infusion of polyvinylester into the nanofiber mat facilitates successful handling of the fragile mats and enables measurements of the dielectric properties. The dielectric constant of the PZT/polyvinylester nanocomposite of about 10% fiber volume fraction was found to be fairly stable and vary from 72 to 62 within the measurement range. The dielectric loss of the composite is below 0.08 at low frequencies and reaches a stable value of 0.04 for most of the measured frequencies.

I. Introduction

LEAD ZIRCONATE TITANATE (PZT) is the most widely used ferroelectric material in ultrasonic transducers, nonvolatile random access memory devices, microelectromechanical devices, sensors, and actuator applications due to its high dielectric constant, high electromechanical coupling coefficient, and large remnant polarization.^{1,2} This material can be processed into various forms such as bulk ceramics, thin films, and fibers, depending on the application area. PZT in fiber form is appealing because of its increased anisotropy and improved flexibility and strength over monolithic PZT ceramics. Micrometer scale PZT fibers are usually incorporated into a polymer matrix to obtain smart piezocomposite structures.³ They can also be used as individual fibers in novel actuator and sensor devices, such as energy harvesting and self-powered *in vivo* medical devices, high-frequency transducers, and nonvolatile ferroelectric memory devices.⁴ Nanoscale PZT fibers are also expected to find wide applications, particularly in nanoelectronics, photonics, sensors, and actuators.⁵

There are a few methods to obtain PZT in fiber form. Sol–gel, viscous suspension spinning process (VSSP), and extrusion, for instance, are applied to produce PZT fibers, typically in the micrometer scale.^{6–8} The electrospinning technique has recently gotten attention because fibers at the micro- and even nanoscale can be produced by this method. Nanoscale PZT fibers have been also produced by the electrospinning method.^{4,9–11} Zhou

*et al.*¹² have produced PZT nanofibers by electrospinning and found that these fibers exhibit significant reversible piezoelectric strains under an applied electric field. The level of this strain was measured to be about 4.2%, which is reportedly six times larger than that observed in thin films.

The objectives of this study are to investigate the processing conditions in the electrospinning of polymeric precursor fiber mats followed by annealing for PZT nanofibers, to examine the phase and morphology of these nanofibers before and after the annealing process, and to characterize the dielectric properties of the resultant PZT/polyvinylester nanocomposite.

II. Experimental Procedure

The PZT sol–gel precursor solution was prepared from lead acetate trihydrate, titanium isopropoxide, and zirconium *n*-butoxide in *n*-butanol. The main solvent used was 2-methoxyethanol. The details of the solution preparation method are shown in Fig. 1(a) and were reported in a previous article.¹³ The final concentration of the precursor sol–gel solution was 0.4M, and the Zr/Ti mol ratio was 1:1. Additionally, 5 mol% lead (Pb) excess was added to the precursor solutions to compensate for lead loss during annealing. Different polymers can be used to provide electrospinning of the PZT.^{9–11} Polyvinyl pyrrolidone (PVP) was chosen and added to the sol–gel solution, with ratios ranging from 6 to 34 wt% in this study. These ratios were determined based on some preliminary experiments. Initially, various PVP ratios starting from 1 wt% were studied systematically with small increments until the first fiber formation was observed. A homemade, electrospinning set-up, allowing a computer-controlled PZT/polymer precursor solution flow rate, was used to prepare the green fiber mats. A schematic of the electrospinning set-up is shown in Fig. 1(b). The applied voltage (12 kV) and the distance between the tip of the needle and the collector (10 cm), resulting in an electrostatic field of 1.2 kV/cm, were kept fixed after preliminary screening experiments. The size of the needle was 300 μm and the pumping speed was 0.5 mL/h. The same processing conditions were used for all the electrospinning experiments in this study.

The viscosity of the precursor solution and PVP mixture was measured by a Brookfield DVIII+ rheometer (Middleboro, MA) using a cone/plate sample holder. The measurements were taken at various shear rates ranging from 38.4 to 768 sn^{-1} . The viscosity was found to remain stable in this measurement range, and only the results taken at the 76.8 sn^{-1} shear rate were reported in this article. The effect of the associated PVP polymer solution concentration was investigated on the morphology of the green precursor fibers. The effect of aging the precursor solution on the morphology of green fibers was also investigated by electrospinning the fiber mats from solutions with a 22 wt% PVP content stored for various periods. The solutions were stored in closed containers to prevent evaporation during the aging process. The viscosity of the aged solutions was recorded before the electrospinning.

Green fibers were sintered in air at 700°C with two different heating rates (0.5° or 5°C/min). Thermogravimetric analysis

S. Danforth—contributing editor

Manuscript No. 25646. Received December 16, 2008; approved June 11, 2009. This work was supported by The Scientific and Technological Research Council of Turkey, TÜBİTAK Grant 106M364, and Turkish Academy of Sciences.

[†]Author to whom correspondence should be addressed. e-mail: ebrualkoy@gmail.com

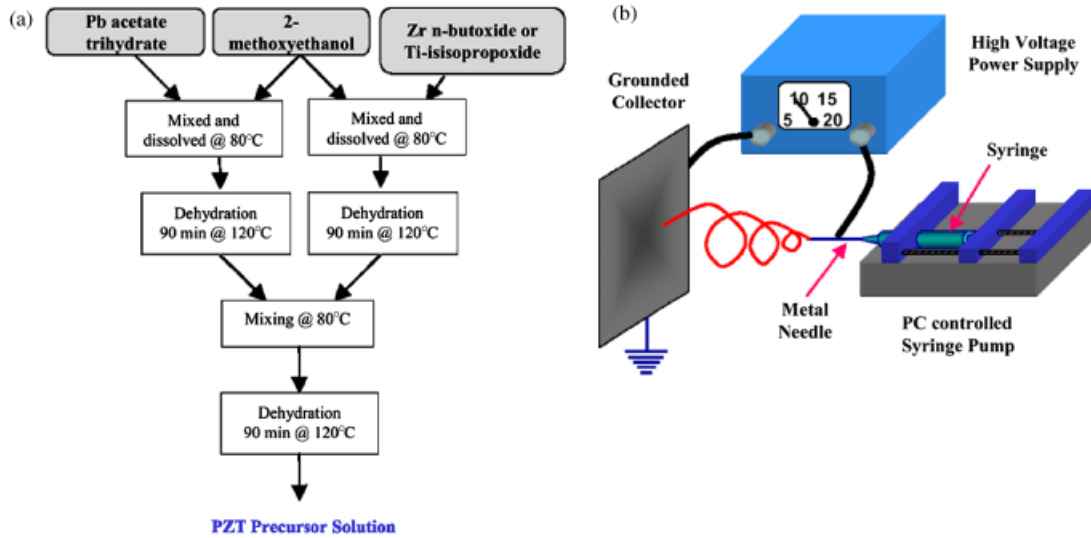


Fig. 1. (a) The process flow chart of precursor sol-gel lead zirconate titanate (PZT) solutions. (b) A schematic of the electrospinning set-up.

(TGA) was used to identify the crucial steps in the pyrolysis and sintering processes.

After obtaining the PZT fiber mats, PZT/polyvinylester composite samples were prepared. T676NA vinyl ester, Accelerator D (styrene 10 wt%, *N-N* dimethylaniline with >89 wt%), Accelerator G (styrene >80 wt%), and Butanox LPT (methyl-ethyl ketone peroxide in diisobutyl phthalate) were mixed to obtain the polymer matrix of the composite. This solution was poured on to the sintered PZT fiber mat and this sample was kept under vacuum for 5 min to eliminate trapped air. Then, the sample was dried 10 h at room temperature.

Sintered mats were characterized by X-ray diffraction (XRD) and scanning electron microscopy (SEM). The dielectric constant and loss of the PZT/polyvinylester composites were measured from 10 kHz to 1 MHz using an HP 4194A Impedance Analyzer (Santa Clara, CA). The samples were prepared into thin, rectangular, parallel plates, and the dielectric measurements were taken by placing the samples between two parallel metal plates of the sample holder.

III. Results and Discussion

(1) Microstructural Features of Green Fiber Mats

The microstructure and the average fiber diameter of the as-prepared green and sintered nanofiber mats were examined by

SEM. Figure 2 shows the microstructure of PZT/PVP green mats at various PVP contents in the solution. From Figs. 2(a) and (b), a small amount of PVP, such as 6 or 12 wt%, was clearly seen to be insufficient to facilitate the fiber formation. On the other hand, the concentration of PVP polymer in the solution exceeding 22 wt% appears to result in a fibrous mat with a reasonable amount of beads (Fig. 2(c)). In particular, bead-free uniform green PZT/PVP fibers of ~ 230 nm in fiber diameter were collected using the 28 wt% PVP ratio solution with a viscosity of 290 mPa. These conditions were considered as optimal in this study (Fig. 2(d)). A further increase of the PVP content to 34 wt% resulted in a smaller fiber diameter, but with the extensive formation of large beads (Fig. 2(e)).

Additional viscosity measurements and investigations were carried out on the PZT precursor solution of 22 wt% PVP considered to be the lower limit for reasonably dominant fiber formation as a function of time in order to explore the effect of aging. Figure 3 shows the diameter of the PZT/PVP green fibers and viscosity of the precursor solution as a function of aging time. It is clearly seen from Figs. 2(c) and (f), along with Fig. 3, that the viscosity of the solution has a significant effect on the formation of fibers and the fiber diameter. Another important and supporting correlation was also observed between the viscosity and the PVP content. The viscosity of the as-prepared (2 h mixed) solution was measured as 140 mPa (Fig. 3). The average

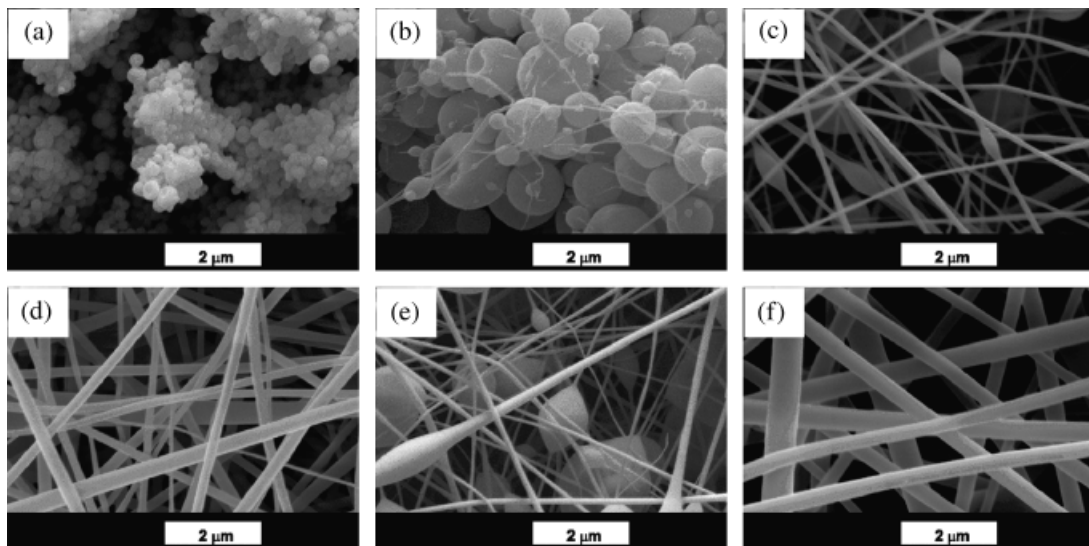


Fig. 2. Lead zirconate titanate (PZT)/polyvinyl pyrrolidone (PVP) green fibers from as-prepared solution with (a) 6 wt%, (b) 12 wt%, (c) 22 wt%, (d) 28 wt%, (e) 34 wt% PVP content. (f) PZT/PVP green fibers from 72-h aged solution with 22 wt% PVP content.

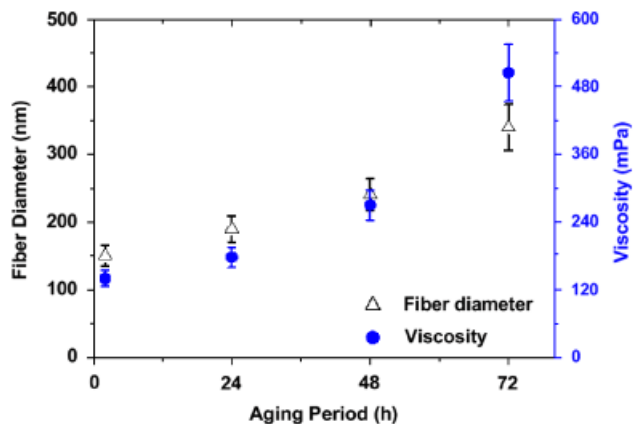


Fig. 3. Variation of the fiber diameter and solution viscosity with aging.

fiber diameter of the mats electrospun from this solution was determined to be 150 nm; however, a beaded structure was observed in these mats (Fig. 2(c)).

The viscosity of the same solution was recorded and nanofiber mats were electrospun after 24, 48, and 72 h of aging. From the SEM examinations of these mats, a bead-free mat structure was obtained from the 48- and 72-h aged solutions. The viscosity of the 48-h aged solution was measured as 270 mPa (Fig. 3) and the average fiber diameter of the mats electrospun from this solution was determined to be 240 nm. When compared with the optimum conditions determined from the solution with a 28 wt% PVP content (viscosity = 290 mPa; fiber diameter = 230 nm), a remarkable correlation was observed. That is, the PVP content of the solution is important to obtain bead-free fiber mats, but the real controlling factor appears to be the viscosity of the polymer solution. The PVP content is believed to be merely ad-

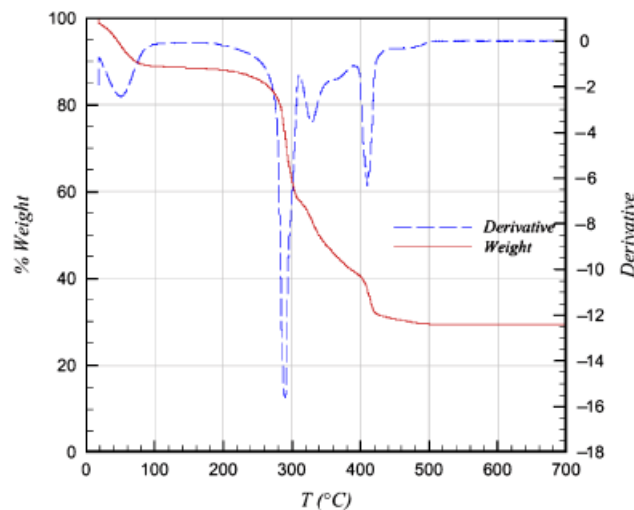


Fig. 4. Thermogravimetric Analysis analysis of the green fiber mats.

justing the viscosity of the solution. The change in the viscosity of the solutions as a result of aging is thought to be due to partial evaporation of the solvent in the polymer solution and the formation of chain-like polymeric particles, which increases the viscosity of the solution. A similar effect of solution aging was observed in a previous study.¹⁴

(2) Structure and Microstructural Features of the Sintered PZT Fibers

TGA of the green fiber mats was performed in order to identify thermal transitions and determine an appropriate annealing regime. From the TGA pattern in Fig. 4, a large amount of weight

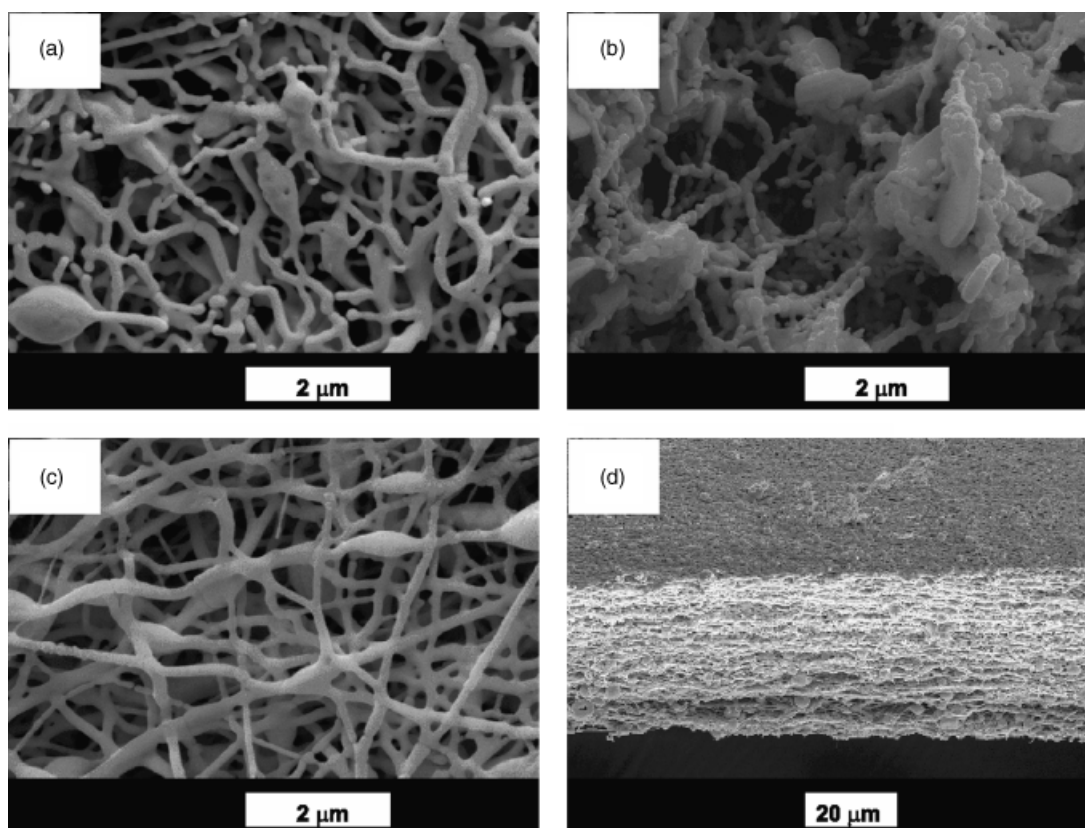


Fig. 5. The micrographs of nanofiber mats prepared from solutions with various polyvinyl pyrrolidone (PVP) contents and sintered at 700°C for 1 h with various heating regimes: (a) 22 wt% PVP and 0.5°C/min, (b) 22 wt% PVP and 5°C/min, (c) 28 wt% PVP and 0.5°C/min. (d) Cross-sectional view of the sintered mat (22 wt% PVP and 0.5°C/min).

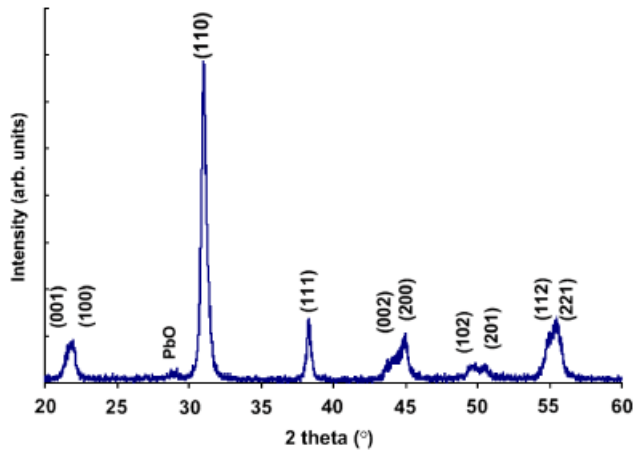


Fig. 6. X-ray diffraction pattern of the lead zirconate titanate nanofiber mat prepared from solution with 28 wt% polyvinyl pyrrolidone content and sintered at 700°C for 1 h.

loss was observed at 290° and 420°C. These temperatures were deemed critical in the sintering of the fiber mats.

PZT fiber mats were annealed at 700°C for 1 h; however, two different annealing regimes (heating rate = 0.5° or 5°C/min) were investigated in accordance with the TGA results. The investigation of the sintering process was initially carried out on green fiber mats from the solution with a 22 wt% PVP content. In the slow heating regime (0.5°C/min), sufficient time was allowed for all organics to be systematically removed, leaving behind a relatively more uniform microstructure (Fig. 5(a)). In contrast, the fast heating regime (5°C/min) yields a more complex microstructure in which, especially, the morphology of the beads was different (Fig. 5(b)). It was observed that the heating

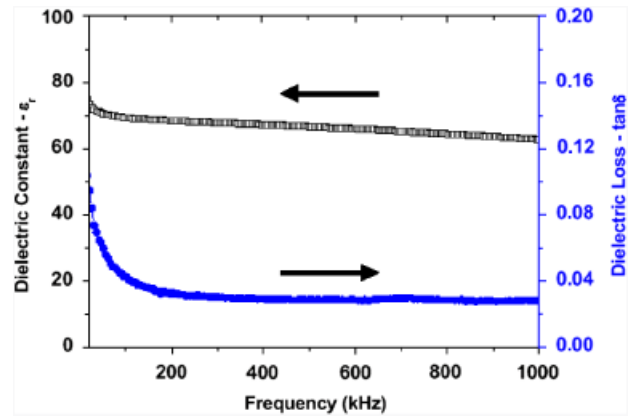


Fig. 8. Dielectric constant and loss of the lead zirconate titanate (PZT)/polyvinylester sample as a function of frequency at room temperature.

regime was influential on the microstructure. This was attributed to the rushed removal of the organic constituents. The mats produced from the solution with a 28 wt% PVP content also yielded a similar microstructure (Fig. 5(c)). The cross-section of the fiber mats is shown in Fig. 5(d). Shrinkage of approximately 40% was recorded on the fiber diameter after sintering.

The phase identification of the sintered PZT nanofibers was performed using XRD. The XRD pattern of the PZT fibers annealed at 700°C for 1 h indicates that these nanofibers are crystallized in the perovskite phase with no preferred orientation and with a small presence of lead oxide (Fig. 6). It is not possible to clearly identify from this pattern whether the PZT is crystallized with a tetragonal or a rhombohedral perovskite phase as a result of the lower annealing temperature of 700°C. However, when the PZT powders prepared from the same sol-gel solu-

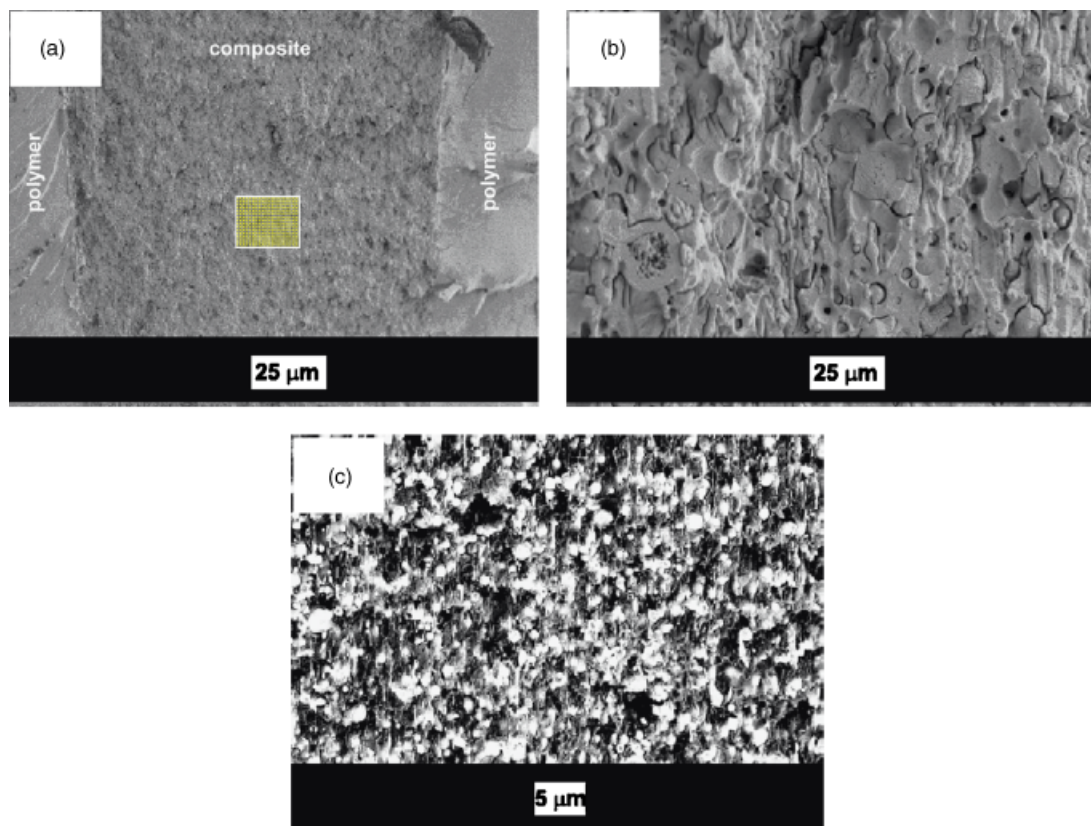


Fig. 7. (a) Cross-sectional microstructure of lead zirconate titanate (PZT)/polyvinylester composite. (b) Higher magnification of the rectangular section of (a). (c) Backscattering electron SEM image of the composite section (PZT nanofiber mat was prepared from solution with 28 wt% polyvinyl pyrrolidone content and sintered at 700°C for 1 h with a 0.5°C/min heating rate).

tion were pressed into pellets and sintered at 1260°C, a clear tetragonal peak splitting was observed at the (100)/(001) and (200)/(002) peaks.⁸

(3) Dielectric Properties of the PZT Nanofiber/Polymer Nanocomposites

After fabricating the PZT fiber mats, PZT/polyvinylester composite samples were prepared. Polyvinylester was tried as the first polymer matrix material in this study. The effect of other matrix materials on the electrical properties will be investigated as a future work. The SEM micrograph of the composite structure is shown in Fig. 7. When the microstructure of the mat is examined at a higher magnification (the section marked with a rectangle in Fig. 7(a)), it is clearly visible from Fig. 7(b) that the polymer matrix phase was infiltrated thoroughly into the fiber network, and an intimate mixture of two phases was obtained. Figure 7(c) shows the backscattering electrons SEM image of the composite section, in which the PZT phase consisting of beads and fibers is visible with a bright-white contrast, and the polyvinylester phase is identifiable as the darker-gray regions. Using Newnham's convention on connectivity of piezocomposites,¹⁵ the composite has 3–3 connectivity, in which the active PZT and the passive polymer matrix phases are both connected in three dimensions in the micrometer scale.

The dielectric constant, ϵ' , of the 3–3 composite was found to be fairly stable and vary from 72 to 62 within the measurement range (Fig. 8). This value is more than an order of magnitude higher than the dielectric constant of the polyvinylester, which was measured as 3.2 in this study. This is due to the increasing contribution of PZT to the dielectric properties of the composites, because undoped PZT has a substantially higher dielectric constant (800 at 1 kHz)¹⁶ than the polymer. Here, the dielectric constant of undoped PZT is taken as a reference point, because doping elements affect the dielectric properties of PZT substantially. In our case, a doping element has not been used in the preparation of the PZT precursor solutions.

The polymer phase in the composite was burnt out at 500°C, and the weight of the sample was recorded before and after the treatment. From the theoretical density of PZT and polymer phases, the volume fraction of the PZT fibers in this composite structure was determined to be about 10%. Using the rule of mixtures

$$\epsilon'_{\text{composite}} = \epsilon'_{\text{polymer}} \times V_{\text{polymer}} + \epsilon'_{\text{PZT}} \times V_{\text{PZT}}$$

and the dielectric constants of the constituent phases, polyvinylester (3.2 at 1 kHz) and undoped PZT (800 at 1 kHz),¹⁶ the dielectric constant of the composite was calculated as 83.2. This calculated value is higher than the measured value. The difference is attributed to the presence of porosity and its contribution to the dielectric constant of the composite. A similar effect has been reported in the literature on 0–3 composites of PZT particles in a polyvinylidene-trifluoroethylene (PVDF-TrFE) copolymer matrix.¹⁷

The dielectric loss of the composite is below 0.08 at low frequencies and reaches a stable value of 0.04 for most of the measured frequencies.

IV. Conclusions

PZT nanofibers were successfully produced by a sequence of electrospinning and sintering processes. Processing conditions, especially the aging of the precursor solution, were found to be critical to the morphology of the green fiber mats. Aging was observed to lead to increased viscosity and a correlated increase in green fiber diameter. Moreover, the annealing regime was found to have a significant influence on the morphology of the sintered nanofiber mats, with slow heating leading to a more uniform morphology. 3–3 composites were prepared from the PZT fiber mats, at about 10% fiber volume fraction, by infiltrating a polyvinylester polymer into the mat. The dielectric constant of the composite measured at room temperature is more than an order of magnitude higher than the polymer matrix and reasonably agrees with the prediction from the rule of mixtures.

References

1. R. Maeda, J. J. Tsaur, S. H. Lee, and M. Ichiki, "Piezoelectric Microactuator Devices," *J. Electroceram.*, **12**, 89–100 (2004).
2. N. Setter and R. Waser, "Electroceraic Materials," *Acta Mater.*, **48**, 151–78 (2000).
3. J. Ouellette, "How Smart Are Smart Materials," *Ind Physicist*, **2** [4] 10–3 (1996).
4. S. Xu, Y. Shi, and S. Kim, "Fabrication and Mechanical Property of Nano Piezoelectric Fibers," *Nanotechnology*, **17**, 4497–501 (2006).
5. X. Y. Zhang, X. Zhao, C. W. Lai, X. G. Tang, and J. Y. Dai, "Synthesis and Piezoresponse of Highly Ordered Pb(Zr_{0.53}Ti_{0.47})O₃ Nanowire Arrays," *Appl. Phys. Lett.*, **85**, 4190–2 (2004).
6. U. Selvaraj, A. V. Prasadarao, S. Komarneni, K. Brooks, and S. Kurtz, "Sol-Gel Processing of PbTiO₃ and Pb(Zr_{0.52}Ti_{0.48})O₃ Fibres," *J. Mater. Res.*, **7**, 992–6 (1992).
7. R. B. Cass, "Fabrication of Continuous Ceramic Fiber by the Viscous Suspension Spinning Process," *Am. Ceram. Soc. Bull.*, **70** [3] 424–9 (1991).
8. J. Heiber, A. Belloli, P. Ermanni, and F. Clemens, "Ferroelectric Characterization of Single PZT Fibers," *J. Int. Mater. Sys. Struct.*, **20**, 379–85 (2009).
9. Y. Wang, R. Furlan, I. Ramos, and J. J. Santiago-Aviles, "Synthesis and Characterization of Micro/Nanosopic Pb(Zr_{0.52}Ti_{0.48})O₃ Fibers by Electrospinning," *Appl. Phys. A*, **78**, 1043–7 (2004).
10. N. Dharmaraj, C. H. Kim, and H. Y. Kim, "Pb(Zr_{0.5}Ti_{0.5})O₃ Nanofibres by Electrospinning," *Mater. Lett.*, **59**, 3085–9 (2005).
11. W. Sigmund, J. Yuh, H. Park, V. Maneeratana, G. Pyrgiotakis, A. Daga, J. Taylor, and J. C. Nino, "Processing and Structure Relationships Electrospinning of Ceramic Fiber Systems," *J. Am. Ceram. Soc.*, **89** [2] 395–407 (2006).
12. Z. H. Zhou, X. S. Gao, J. Wang, K. Fujihara, S. Ramakrishna, and V. Nagarajan, "Giant Strain in Pb(Zr_{0.2}Ti_{0.8})O₃ Nanowires," *Appl. Phys. Lett.*, **90**, 052902 (2007).
13. E. Mensur Alkoy, S. Alkoy, and T. Shiosaki, "Microstructure and Crystallographic Orientation Dependence of Electrical Properties in Lead Zirconate Thin Films Prepared by Sol-Gel Process," *Jpn. J. Appl. Phys.*, **44** [12] 8606–12 (2005).
14. E. Mensur Alkoy, S. Alkoy, and T. Shiosaki, "The Effect of Crystallographic Orientation and Solution Aging on the Electrical Properties of Sol-Gel Derived Pb(Zr_{0.45}Ti_{0.55})O₃ Thin Films," *Ceram. Int.*, **33**, 1455–62 (2007).
15. R. E. Newnham, D. P. Skinner, and L. E. Cross, "Connectivity and Piezoelectric-Pyroelectric Composites," *Mater. Res. Bull.*, **13** [5] 525–36 (1978).
16. B. Lee and E. J. Lee, "Effects of Complex Doping on Microstructural and Electrical Properties of PZT Ceramics," *Electroceraic*, **17** [2–4] 597–602 (2006).
17. M. Dietze and M. Es-Souni, "Structural and Functional Properties of Screen-Printed PZT-PVDF-TrFE Composites," *Sens. Actuators A*, **143**, 329–34 (2008). □